

Production and Elliptic Flow of Dileptons and Photons in the semi-Quark Gluon Plasma

Charles Gale,^{1,2} Yoshimasa Hidaka,³ Sangyong Jeon,¹ Shu Lin,⁴ Jean-François Paquet,¹
Robert D. Pisarski,^{5,4} Daisuke Satow,^{3,5} Vladimir V. Skokov,⁶ and Gojko Vujanovic¹

¹*Department of Physics, McGill University, 3600 University Street, Montreal, QC H3A 2T8, Canada*

²*Frankfurt Institute for Advanced Studies, Ruth-Moufang-Str. 1, D-60438 Frankfurt am Main, Germany*

³*Theoretical Research Division, Nishina Center, RIKEN, Wako 351-0198, Japan*

⁴*RIKEN/BNL Research Center, Brookhaven National Laboratory, Upton, NY 11973, USA*

⁵*Department of Physics, Brookhaven National Laboratory, Upton, NY 11973, USA*

⁶*Department of Physics, Western Michigan University,
1903 W. Michigan Avenue, Kalamazoo, MI 49008*

We consider the thermal production of dileptons and photons at temperatures above the critical temperature in QCD. We use a model where color excitations are suppressed by a small value of the Polyakov loop, the semi Quark-Gluon Plasma (QGP). Comparing the semi-QGP to the perturbative QGP, we find a mild enhancement of thermal dileptons. In contrast, to leading logarithmic order in weak coupling there are far fewer hard photons from the semi-QGP than the usual QGP. To illustrate the possible effects on photon and dileptons production in heavy ion collisions, we integrate the rate with a realistic hydrodynamic simulation. Dileptons uniformly exhibit a small flow, but the strong suppression of photons in the semi-QGP tends to bias the elliptical flow of photons to that generated in the hadronic phase.

PACS numbers: 11.10.Wx, 12.38.Mh, 25.75.Cj, 25.75.Nq

The collisions of heavy nuclei at ultra-relativistic energies can be used to investigate the properties of the Quark-Gluon Plasma (QGP). At both the Relativistic Heavy Ion Collider (RHIC) and the Large Hadron Collider (LHC), much of the collision takes place at temperatures which are not that far above that for the transition, T_c . This is a difficult region to study: perturbative methods can be used at high temperature, but not near T_c [1]. Similarly, hadronic models are valid at low temperature, but break down near T_c [2]. One model of the region above but near T_c is the semi-QGP [3–6]. This incorporates the results of numerical simulations on the lattice [7], which show that colored excitations are strongly suppressed when $T \rightarrow T_c^+$, as the expectation value of the Polyakov loop decreases markedly.

A notable property of heavy ion collisions is elliptic flow, how the initial spatial anisotropy of peripheral collisions is transformed into a momentum anisotropy. The large elliptic flow of hadrons can be well modeled by hydrodynamic models in which the QCD medium is close to an ideal fluid [8–10].

Electromagnetic signals, such as dilepton or photon production, are another valuable probe, since they reflect properties of the quark and gluon distributions of the QGP, and once produced, escape without significant interaction [11–24]. For example, if most photons are emitted at high temperature in the QGP, since the flow at early times is small, one would expect a small net elliptic flow for photons. However, recently both the PHENIX experiment at RHIC [22] and the ALICE experiment at the LHC [23] have found a large elliptic flow for photons, comparable to that of hadrons. This is most puzzling [17, 18, 24].

In this paper we present the results for the thermal

production of hard dileptons and photons in the semi-QGP, and compare them with those of the perturbative QGP. Surprisingly, we find a sharp qualitative difference between the two. In the semi-QGP, the production of dileptons is similar between the deconfined and confined phases, while photon production is *strongly* suppressed near T_c . We compute to leading order in the QCD coupling (for photons, only to leading logarithmic order) and give complete results later [25]. We then use a hydrodynamic model [16] to compute the effect on the number of dileptons and photons produced, and on the elliptic flow, v_2 . The effects on thermal dileptons are modest. The suppression of thermal photons near T_c in the semi-QGP, though, implies that v_2 is biased towards that generated in the hadronic phase. Our results may help to understand the puzzle of the elliptic flow for photons.

Deconfinement in a $SU(N_c)$ gauge theory is characterized by the Polyakov loop, $\ell = (1/N_c)\text{tr} \mathcal{P} \exp(ig \int_0^{1/T} d\tau A_0)$, where \mathcal{P} denotes path ordering, T is the temperature, g the gauge coupling constant, and A_0 the temporal component of the gauge field. At high temperature $\langle \ell \rangle \sim 1$ [26], while $\langle \ell \rangle = 0$ in the confined phase of a pure gauge theory. With dynamical quarks, $\langle \ell \rangle > 0$ at any nonzero temperature, but lattice simulations show that the value of the (renormalized) loop is small at T_c , $\langle \ell(T_c) \rangle \approx 0.1$ [7].

The simplest way to represent a phase where $\langle \ell \rangle < 1$ is to work in mean field theory, taking A_0 to be a constant, diagonal matrix, $(A_0^{cl})^{ab} = \delta^{ab} Q^a/g$ [3–6]. The Polyakov loop is then $\ell = 1/N_c \sum_a e^{iQ^a/T}$, where the color index $a = 1 \dots N_c$. For three colors, $A_0^{cl} = (Q, -Q, 0)/g$, so $Q = 2\pi T/3$ in the confined vacuum, $\ell = 0$. Since $A_0^{cl} \sim T/g$, this is manifestly a model of non-perturbative

physics.

In Minkowski spacetime, the diagrams are those of ordinary perturbation theory, except that the background field A_0^c acts like an imaginary chemical potential for color. For a quark with color a , the Fermi-Dirac distribution function is $1/(e^{(E-iQ^a)/T} + 1)$. In the double line basis gluons carry two color indices, (ab) , and their Bose-Einstein distribution function involves a difference of Q 's, $1/(e^{(E-i(Q^a-Q^b))/T} - 1)$. In the Boltzmann approximation, the distribution function for a single quark (or anti-quark), summed over color, is suppressed by the Polyakov loop, $\sim \sum_a e^{-(E-iQ^a)/T}/N_c \sim e^{-E/T} \ell$; for gluons, it is $\sim e^{-E/T} \ell^2$.

In the semi-QGP model, one computes to leading order in the QCD coupling with $Q^a \neq 0$ [3–6]. We first discuss the results for thermal dilepton production. Let the sum of the momenta of the dilepton be $P^\mu = (E, \vec{p})$, $p = |\vec{p}|$, where $E > p$. To leading order in perturbation theory, this arises from the annihilation of a quark anti-quark pair into a virtual photon, which then decays into a dilepton pair. For three colors and $Q = 0$, the production rate [16] is

$$\left. \frac{d\Gamma}{d^4P} \right|_{Q=0} = \frac{\alpha_{em}}{6\pi^4} n(E) \left(1 - \frac{2T}{p} \ln \frac{1 + e^{-p_-/T}}{1 + e^{-p_+/T}} \right); \quad (1)$$

$p_\pm = (E \pm p)/2$, and $n(E) = 1/(e^{E/T} - 1)$ is the usual Bose-Einstein distribution function. This includes the contributions of (massless) up, down and strange quarks, where $\alpha_{em} = e^2/4\pi$, and e is the electromagnetic coupling constant.

In the semi-QGP, to leading order the result when $Q \neq 0$ is a simple factor times that for $Q = 0$ [25],

$$\left. \frac{d\Gamma}{d^4P} \right|_{Q \neq 0} = f_{ll}(Q) \left. \frac{d\Gamma}{d^4P} \right|_{Q=0}, \quad (2)$$

where $f_{ll}(Q) \equiv \tilde{f}_{ll}(Q)/\tilde{f}_{ll}(0)$. For three colors, this can be written in terms of the Polyakov loop,

$$\tilde{f}_{ll} = 1 - \frac{2T}{3p} \ln \frac{1 + 3\ell e^{-p_-/T} + 3\ell e^{-2p_-/T} + e^{-3p_-/T}}{1 + 3\ell e^{-p_+/T} + 3\ell e^{-2p_+/T} + e^{-3p_+/T}}. \quad (3)$$

In the special case that the dileptons move back to back, $p = 0$, we plot the modification factor at $E = 1$ GeV as a function of temperature in Fig. (1), taking the Q^a 's from Ref. [6]. We find that $f_{ll}(Q)$ is always greater than one.

To understand this, remember that in kinetic theory the production rate for dileptons is the product of statistical distribution functions times an amplitude. When $p = 0$, the distribution functions are for a quark with energy $E/2$ and color a , and an anti-quark, also with energy $E/2$ and color a . If the total energy $E \gg T$, we can use the Boltzmann approximation for the Q^a -dependent Fermi-Dirac distribution functions,

$$e^2 \sum_{a=1}^N e^{-(E/2-iQ^a)/T} e^{-(E/2+iQ^a)/T} |\mathcal{M}_{ll}|^2. \quad (4)$$

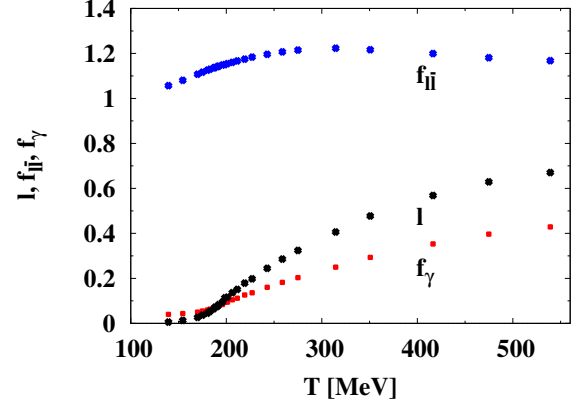


FIG. 1. The ratio of the thermal production of dileptons and photons in the semi-QGP, versus that in perturbation theory, as a function of temperature. For dileptons, f_{ll} from Eq. (3) is for $E = 1$ GeV and $p = 0$. For photons, f_{γ} in Eq. (7) is independent of the photon momentum. The loop is taken from Ref. [6].

As the Q^a 's are like a chemical potential for color, they enter the distribution functions for the quark and anti-quark with *opposite* signs, and so at large energy, cancel identically. That is, the probability for a hard virtual photon to produce a quark anti-quark pair is independent of the Q^a 's, and so the Polyakov loop. This is in stark contrast to the statistical distribution function for a *single* quark or anti-quark, which is $\sim \ell$.

Fig. (1) shows that for moderate values of $E \sim T$, there are corrections to the Boltzmann approximation which even give a modest *enhancement* above T_c , by about $\sim 20\%$.

Expanding Eq. (3) to quadratic order in the Q^a is equivalent to considering a condensate $\sim \langle \text{tr } A_0^2 \rangle$, and agrees with previous results [13]. Ref. [13] suggested that an enhancement like that which we find could explain the excess of dileptons found below the ρ meson mass in heavy ion collisions; see, also, Ref. [12, 15].

We now consider the production of real photons at a large momentum P^μ , where $E = p \gg T$. To leading order in the QCD coupling, apparently two processes contribute to photon production: Compton scattering of a quark or anti-quark, and the pair annihilation of a quark and an anti-quark. These $2 \rightarrow 2$ processes [11] are both $\sim e^2 g^2$. However, a quark which scatters with an arbitrary number of soft gluons, with $E_{\text{soft}} \sim gT$, emits collinear photons at the same order, $\sim e^2 g^2$. [14]. This depends crucially upon Bose-Einstein enhancement for the soft gluon, as $n(E_{\text{soft}}) \sim 1/g$.

In the semi-QGP, however, there is no Bose-Einstein enhancement for off-diagonal gluons: at small E the gluon distribution function is $\sim 1/(e^{-i(Q^a-Q^b)/T} - 1)$, if $a \neq b$ and $Q^a - Q^b \sim T$. There is Bose-Einstein enhancement for soft, diagonal gluons, where $a = b$, but at large N_c there are only $\sim N_c$ diagonal gluons to $\sim N_c^2$ off-

diagonal gluons. Consequently up to corrections $\sim 1/N_c$, in the semi-QGP the production of real photons is dominated by $2 \rightarrow 2$ processes. This is a straightforward generalization of the original computations of Ref. [11]. The results for collinear emission at large N_c will be given later [25].

Computing thermal photon production only to leading logarithmic order, we find [25]

$$E \frac{d\Gamma}{d^3p} \Big|_{Q \neq 0} = f_\gamma(Q) E \frac{d\Gamma}{d^3p} \Big|_{Q=0}. \quad (5)$$

At the same order, the result for $2 \rightarrow 2$ scattering in the perturbative regime [11] is

$$E \frac{d\Gamma}{d^3p} \Big|_{Q=0} = \frac{\alpha_{em}\alpha_s}{3\pi^2} e^{-E/T} T^2 \ln \left(\frac{E}{g^2 T} \right), \quad (6)$$

where $\alpha_s = g^2/(4\pi)$, and

$$f_\gamma(Q) = 1 - 4q + \frac{10}{3} q^2; \quad q = \frac{Q}{2\pi T}, \quad 0 < q < 1. \quad (7)$$

In the perturbative limit, $f_\gamma(0) = 1$. This function decreases monotonically as Q increases, with $f_\gamma(2\pi T/3) = 1/27$ in the confined phase. In Fig. (1) we plot f_γ versus temperature. This result is independent of momentum when $E \gg T$.

Why photon production is strongly suppressed in the confined phase can be understood from the case of pair annihilation. Using kinetic theory in the Boltzmann approximation, photon production is proportional to

$$e^2 g^2 \sum_{a,b} e^{-(E_1 - iQ^a)/T} e^{-(E_2 + iQ^b)/T} |\mathcal{M}_\gamma^{ab}|^2, \quad (8)$$

where E_1 is the energy of the incoming quark with color a , E_2 the energy of the anti-quark with color b , and \mathcal{M}_γ^{ab} a matrix element, which depends upon a and b . The quark and anti-quark then scatter into a gluon, with color indices (ab) , and a photon. In the deconfined phase, the rate is $\sim e^2 g^2 N_c^2$. In the confined phase, however, to avoid suppression by powers of the Polyakov loop the color charges of the quark and anti-quark must match up, with $a = b$. This reduces the result by one factor of $1/N_c$. Further, the matrix element \mathcal{M}_γ^{ab} involves the quark-gluon vertex; when $a = b$, this gives another factor of $1/N_c$, for an overall factor of $1/N_c^2$. The same counting in $1/N_c$ applies for Compton scattering. In all, at large N_c the ratio of hard photon production in the confined phase, to that in the deconfined phase, is $f_\gamma = 1/(3N_c^2)$ [25]. Even for three colors this is a rather small number, $1/27$.

Moving towards a qualitative estimate of the effects upon experiment, we multiply the full photon emission rate to $\sim e^2 g^2$ [14] by the suppression factor which we find to leading logarithmic order, $f_\gamma(Q)$ in Eq. (7). We use MUSIC, a 3+1 D hydrodynamic simulation [9, 10]. As the purpose of this study is to determine the global effect of rates in the semi-QGP, versus that in the usual

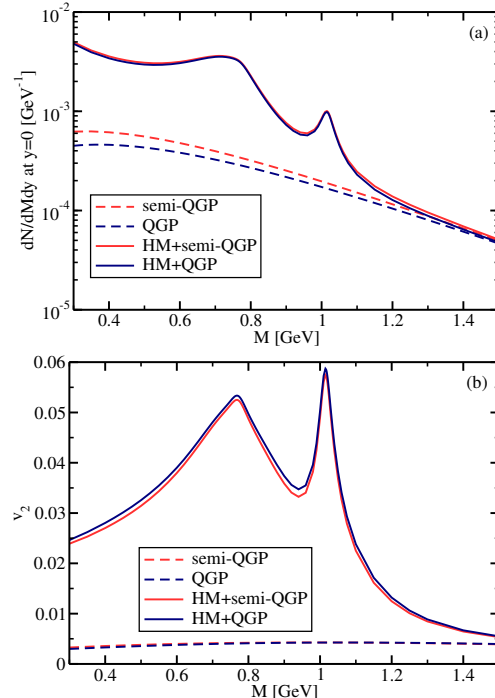


FIG. 2. Dilepton yield (a) and elliptic flow (b) computed using MUSIC, from the semi-QGP and QGP, plus hadronic matter (HM). This calculation is for Au+Au collisions at the top RHIC energy, $\sqrt{s} = 200 \text{ GeV}/A$, in the 20-40% centrality class.

QGP, we also include the hadronic rates for dileptons [16] and photons [15]. We use ideal hydrodynamics for nucleus-nucleus collisions, with $A = 200$ at RHIC energies, $\sqrt{s_{NN}} = 200 \text{ GeV}$.

In ideal hydrodynamics, fluid dynamics is governed by the conservation equation for the stress-energy tensor, $\partial_\mu T^{\mu\nu} = 0$, where $T^{\mu\nu} = (\varepsilon + P)u^\mu u^\nu - g^{\mu\nu}P$; ε is the energy density, P the thermodynamic pressure and u^μ the fluid four-velocity. The details regarding the numerical algorithm being used to solve the hydrodynamic equations along with the initial and freeze-out conditions are presented in Ref. [9].

Fig. (2) shows the results for the dileptons. There are slightly more dileptons from the semi-QGP than the usual QGP, but below an invariant mass of 1.5 GeV, the total yield is dominated by the hadronic matter. It might be possible to detect dileptons from the semi-QGP above 1.5 GeV. The dilepton elliptic flow is small, $v_2 \sim 0.01 - 0.06$, and is dominated by that from hadronic matter.

The results for photons, shown in Fig. (3), are very different. The suppression of color in the semi-QGP greatly reduces the photon yield, Fig. (3a). The v_2 of the semi-QGP is also reduced with respect to that of the QGP, Fig. (3b).

However, the *total* thermal photon v_2 is a yield-weighted average of the v_2 from the QGP and hadronic

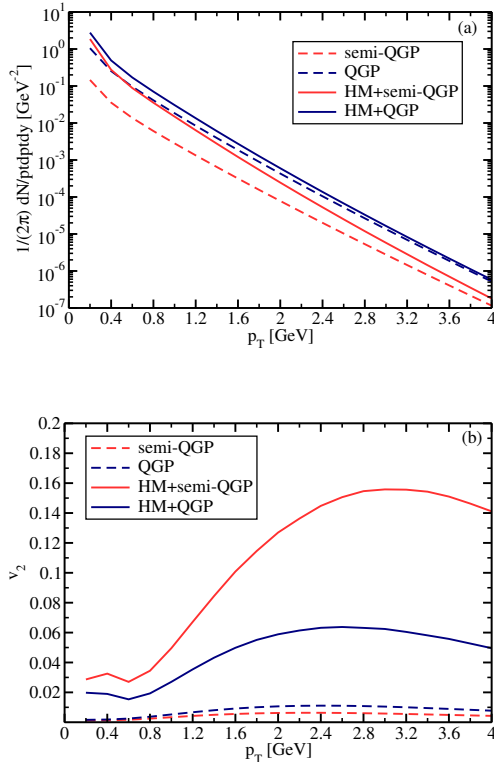


FIG. 3. Photon yield (a) and elliptic flow (b) using MUSIC, from the semi-QGP and QGP, plus hadronic matter (HM). As in Fig. (3), this calculation is for Au+Au collisions at the top RHIC energy, in the 20-40% centrality class.

phases. There is a competition between the change in the QGP yield and that of v_2 : lowering the QGP v_2 lowers the thermal photon v_2 , while a decrease in the yield from the QGP biases the thermal photon v_2 towards that from the hadronic phase, which is large. From Fig. (3b), the latter wins, so that using semi-QGP rates significantly increases the total v_2 for thermal photons.

To make a detailed comparison to experiment, it is crucial to take into account the contribution of prompt photons, produced through the collisions of hard partons. Prompt photons can be computed using perturbative QCD, which work well in proton-proton collisions at next to leading order [27]. The dominant uncertainties of the perturbative calculation are the limited knowledge

of the parton fragmentation functions into photons, and the dependence on the renormalization mass scale [20].

There are further difficulties in extrapolating the contribution of prompt photons from proton-proton to heavy ion collisions. Parton distribution functions are nuclear dependent, but more importantly, parton fragmentation functions are medium-dependent [21]. Photons with low p_T are produced predominantly by parton fragmentation. In heavy ion collisions, experimentally it is found that hadrons with p_T up to ≈ 10 GeV exhibit large elliptic flow. Thus a photon produced by the fragmentation of a hard jet should inherit at least some of the elliptic flow of that jet.

Lastly, in heavy ion collisions at moderate p_T , the number of photons produced by both perturbative and thermal mechanisms appear to be significantly below that observed experimentally. This may be due to an underestimate of rates in the hadronic medium [12] or to photons produced in the initial state, such as from the Color Glass Condensate [18].

Previous computations in the semi-QGP show that like photon production, processes involving color excitations, such as the shear viscosity [4] and the collisional energy loss of heavy quarks [6], are strongly suppressed near T_c . Thus we expect that the radiative energy loss of light quarks, which involves the Landau-Pomeranchuk-Migdal effect, is strongly suppressed near T_c . Such computations are presently underway.

ACKNOWLEDGMENTS

We thank H. van Hees, Y.-Q. Ma, L. McLerran, J. Qiu, R. Rapp, B. Schenke, W. Vogelsang, and I. Zahed for useful discussions. C.G., S.J., J.-F.P. and G.V. are supported in part by the Natural Sciences and Engineering Research Council of Canada. Y.H. is partially supported by JSPS KAKENHI Grants Numbers 24740184, and by the RIKEN iTHES Project. S.L. is supported by the RIKEN Foreign Postdoctoral Researchers Program. J.-F.P. and G. V. acknowledge scholarships from Hydro-Quebec, FRQNT, and from the Canadian Institute of Nuclear Physics. R.D.P. is supported by the U.S. Department of Energy under contract #DE-AC02-98CH10886. D. S. is supported by JSPS Strategic Young Researcher Overseas Visits Program for Accelerating Brain Circulation (No. R2411).

-
- [1] N. Haque, A. Bandyopadhyay, J. O. Andersen, M. G. Mustafa, M. Strickland, *et al.*, (2014), [arXiv:1402.6907 \[hep-ph\]](#).
 - [2] P. Huovinen and P. Petreczky, *Nucl.Phys.* **A837**, 26 (2010), [arXiv:0912.2541 \[hep-ph\]](#); A. Andronic, P. Braun-Munzinger, J. Stachel, and M. Winn, *Phys.Lett.* **B718**, 80 (2012), [arXiv:1201.0693 \[nucl-th\]](#).
 - [3] R. D. Pisarski, *Phys.Rev.* **D74**, 121703 (2006),

[arXiv:hep-ph/0608242 \[hep-ph\]](#).

- [4] Y. Hidaka and R. D. Pisarski, *Phys.Rev.* **D78**, 071501 (2008), [arXiv:0803.0453 \[hep-ph\]](#); *Phys.Rev.* **D80**, 036004 (2009), [arXiv:0906.1751 \[hep-ph\]](#); *Phys.Rev.* **D80**, 074504 (2009), [arXiv:0907.4609 \[hep-ph\]](#); *Phys.Rev.* **D81**, 076002 (2010), [arXiv:0912.0940 \[hep-ph\]](#).
- [5] A. Dumitru, Y. Guo, Y. Hidaka, C. P. Korthals Altes,

- and R. D. Pisarski, *Phys.Rev.* **D83**, 034022 (2011), [arXiv:1011.3820 \[hep-ph\]](#); A. Dumitru, Y. Guo, Y. Hidaka, C. P. K. Altes, and R. D. Pisarski, *Phys.Rev.* **D86**, 105017 (2012), [arXiv:1205.0137 \[hep-ph\]](#); K. Kashiwa, R. D. Pisarski, and V. V. Skokov, *Phys.Rev.* **D85**, 114029 (2012), [arXiv:1205.0545 \[hep-ph\]](#); R. D. Pisarski and V. V. Skokov, *Phys.Rev.* **D86**, 081701 (2012), [arXiv:1206.1329 \[hep-th\]](#); K. Kashiwa and R. D. Pisarski, *Phys.Rev.* **D87**, 096009 (2013), [arXiv:1301.5344 \[hep-ph\]](#); S. Lin, R. D. Pisarski, and V. V. Skokov, *Phys.Rev.* **D87**, 105002 (2013), [arXiv:1301.7432 \[hep-ph\]](#).
- [6] S. Lin, R. D. Pisarski, and V. V. Skokov, (2013), [10.1016/j.physletb.2014.01.043](#), [arXiv:1312.3340 \[hep-ph\]](#).
- [7] A. Bazavov, T. Bhattacharya, M. Cheng, N. Christ, C. DeTar, *et al.*, *Phys.Rev.* **D80**, 014504 (2009), [arXiv:0903.4379 \[hep-lat\]](#); C. DeTar and U. Heller, *Eur.Phys.J.* **A41**, 405 (2009), [arXiv:0905.2949 \[hep-lat\]](#); Z. Fodor and S. Katz, (2009), [arXiv:0908.3341 \[hep-ph\]](#); P. Petreczky, *J.Phys.* **G39**, 093002 (2012), [arXiv:1203.5320 \[hep-lat\]](#); S. Borsanyi, Z. Fodor, C. Hoelbling, S. D. Katz, S. Krieg, *et al.*, *Phys.Lett.* **B370**, 99 (2014), [arXiv:1309.5258 \[hep-lat\]](#); T. Bhattacharya, M. I. Buchoff, N. H. Christ, H. T. Ding, R. Gupta, *et al.*, (2014), [arXiv:1402.5175 \[hep-lat\]](#); S. Sharma, *Adv.High Energy Phys.* **2013**, 452978 (2013), [arXiv:1403.2102 \[hep-lat\]](#).
- [8] U. W. Heinz, (2009), [arXiv:0901.4355 \[nucl-th\]](#); U. Heinz and R. Snellings, *Ann.Rev.Nucl.Part.Sci.* **63**, 123 (2013), [arXiv:1301.2826 \[nucl-th\]](#); C. Gale, S. Jeon, and B. Schenke, *Int.J.Mod.Phys.* **A28**, 1340011 (2013), [arXiv:1301.5893 \[nucl-th\]](#).
- [9] B. Schenke, S. Jeon, and C. Gale, *Phys.Rev.* **C82**, 014903 (2010), [arXiv:1004.1408 \[hep-ph\]](#).
- [10] B. Schenke, S. Jeon, and C. Gale, *Phys.Rev.Lett.* **106**, 042301 (2011), [arXiv:1009.3244 \[hep-ph\]](#).
- [11] R. Baier, H. Nakkagawa, A. Niegawa, and K. Redlich, *Z.Phys.* **C53**, 433 (1992); J. I. Kapusta, P. Lichard, and D. Seibert, *Phys.Rev.* **D44**, 2774 (1991).
- [12] J. V. Steele, H. Yamagishi, and I. Zahed, *Phys.Lett.* **B384**, 255 (1996), [arXiv:hep-ph/9603290 \[hep-ph\]](#); *Phys.Rev.* **D56**, 5605 (1997), [arXiv:hep-ph/9704414 \[hep-ph\]](#); J. V. Steele and I. Zahed, *Phys.Rev.* **D60**, 037502 (1999), [arXiv:hep-ph/9901385 \[hep-ph\]](#); K. Dusling, D. Teaney, and I. Zahed, *Phys.Rev.* **C75**, 024908 (2007), [arXiv:nucl-th/0604071 \[nucl-th\]](#); K. Dusling and I. Zahed, *Nucl.Phys.* **A825**, 212 (2009), [arXiv:0712.1982 \[nucl-th\]](#); *Phys.Rev.* **C82**, 054909 (2010), [arXiv:0911.2426 \[nucl-th\]](#).
- [13] C. Lee, J. Wirstam, I. Zahed, and T. Hansson, *Phys.Lett.* **B448**, 168 (1999), [arXiv:hep-ph/9809440 \[hep-ph\]](#).
- [14] P. Aurenche, F. Gelis, and H. Zaraket, *Phys.Rev.* **D62**, 096012 (2000), [arXiv:hep-ph/0003326 \[hep-ph\]](#); P. B. Arnold, G. D. Moore, and L. G. Yaffe, *JHEP* **0206**, 030 (2002), [arXiv:hep-ph/0204343 \[hep-ph\]](#); *JHEP* **0112**, 009 (2001), [arXiv:hep-ph/0111107 \[hep-ph\]](#).
- [15] S. Turbide, R. Rapp, and C. Gale, *Phys.Rev.* **C69**, 014903 (2004), [arXiv:hep-ph/0308085 \[hep-ph\]](#); J. Manninen, E. Bratkovskaya, W. Cassing, and O. Linnyk, *Eur.Phys.J.* **C71**, 1615 (2011), [arXiv:1005.0500 \[nucl-th\]](#); P. Staig and E. Shuryak, (2010), [arXiv:1005.3531 \[nucl-th\]](#); O. Linnyk, W. Cassing, J. Manninen, E. Bratkovskaya, and C. Ko, *Phys.Rev.* **C85**, 024910 (2012), [arXiv:1111.2975 \[nucl-th\]](#); O. Linnyk, W. Cassing, J. Manninen, E. Bratkovskaya, P. Gossiaux, *et al.*, *Phys.Rev.* **C87**, 014905 (2013), [arXiv:1208.1279 \[nucl-th\]](#); R. Rapp, *Adv.High Energy Phys.* **2013**, 148253 (2013), [arXiv:1304.2309 \[hep-ph\]](#); P. M. Hohler and R. Rapp, *Phys.Lett.* **B731**, 103 (2014), [arXiv:1311.2921 \[hep-ph\]](#); C.-H. Lee and I. Zahed, (2014), [arXiv:1403.1632 \[hep-ph\]](#).
- [16] G. Vujanovic, C. Young, B. Schenke, R. Rapp, S. Jeon, and C. Gale, (2013), [arXiv:1312.0676 \[nucl-th\]](#).
- [17] R. Chatterjee, E. S. Frodermann, U. W. Heinz, and D. K. Srivastava, *Phys.Rev.Lett.* **96**, 202302 (2006), [arXiv:nucl-th/0511079 \[nucl-th\]](#); E. Bratkovskaya, S. Kiselev, and G. Sharkov, *Phys.Rev.* **C78**, 034905 (2008), [arXiv:0806.3465 \[nucl-th\]](#); H. van Hees, C. Gale, and R. Rapp, *Phys.Rev.* **C84**, 054906 (2011), [arXiv:1108.2131 \[hep-ph\]](#); G. Basar, D. Kharzeev, and V. Skokov, *Phys.Rev.Lett.* **109**, 202303 (2012), [arXiv:1206.1334 \[hep-ph\]](#); A. Bzdak and V. Skokov, *Phys.Rev.Lett.* **110**, 192301 (2013), [arXiv:1208.5502 \[hep-ph\]](#); K. Fukushima and K. Mameda, *Phys.Rev.* **D86**, 071501 (2012), [arXiv:1206.3128 \[hep-ph\]](#); F.-M. Liu and S.-X. Liu, *Phys.Rev.* **C89**, 034906 (2014), [arXiv:1212.6587 \[nucl-th\]](#); C. Shen, U. W. Heinz, J.-F. Paquet, I. Kozlov, and C. Gale, (2013), [arXiv:1308.2111 \[nucl-th\]](#); C. Shen, U. W. Heinz, J.-F. Paquet, and C. Gale, *Phys.Rev.* **C89**, 044910 (2014), [arXiv:1308.2440 \[nucl-th\]](#); O. Linnyk, V. Konchakovski, W. Cassing, and E. Bratkovskaya, *Phys.Rev.* **C88**, 034904 (2013), [arXiv:1304.7030 \[nucl-th\]](#); O. Linnyk, W. Cassing, and E. Bratkovskaya, *Phys.Rev.* **C89**, 034908 (2014), [arXiv:1311.0279 \[nucl-th\]](#); B. Muller, S.-Y. Wu, and D.-L. Yang, *Phys.Rev.* **D89**, 026013 (2014), [arXiv:1308.6568 \[hep-th\]](#); G. Basar, D. E. Kharzeev, and E. V. Shuryak, (2014), [arXiv:1402.2286 \[hep-ph\]](#); H. van Hees, M. He, and R. Rapp, (2014), [arXiv:1404.2846 \[nucl-th\]](#); A. Monnai, (2014), [arXiv:1403.4225 \[nucl-th\]](#).
- [18] L. McLerran and B. Schenke, (2014), [arXiv:1403.7462 \[hep-ph\]](#).
- [19] M. Dion, J.-F. Paquet, B. Schenke, C. Young, S. Jeon, *et al.*, *Phys.Rev.* **C84**, 064901 (2011), [arXiv:1109.4405 \[hep-ph\]](#).
- [20] M. Klasen, C. Klein-Boesing, F. Knig, and J. Wessels, *JHEP* **1310**, 119 (2013), [arXiv:1307.7034](#); M. Klasen and F. Konig, (2014), [arXiv:1403.2290 \[hep-ph\]](#).
- [21] F. Arleo, *JHEP* **0609**, 015 (2006), [arXiv:hep-ph/0601075 \[hep-ph\]](#); *Eur.Phys.J.* **C61**, 603 (2009), [arXiv:0810.1193 \[hep-ph\]](#); F. Arleo, K. J. Eskola, H. Paukkunen, and C. A. Salgado, *JHEP* **1104**, 055 (2011), [arXiv:1103.1471 \[hep-ph\]](#).
- [22] A. Adare *et al.* (PHENIX Collaboration), *Phys.Rev.Lett.* **109**, 122302 (2012), [arXiv:1105.4126 \[nucl-ex\]](#).
- [23] D. Lohner (ALICE), *J.Phys.Conf.Ser.* **446**, 012028 (2013), [arXiv:1212.3995 \[hep-ex\]](#).
- [24] T. Sakaguchi, (2014), [arXiv:1401.2481 \[nucl-ex\]](#).
- [25] Y. Hidaka, S. Lin, R. D. Pisarski, and D. Satow, in preparation (2014).
- [26] E. Gava and R. Jengo, *Phys.Lett.* **B105**, 285 (1981); Y. Burnier, M. Laine, and M. Vepsalainen, *JHEP* **1001**, 054 (2010), [arXiv:0911.3480 \[hep-ph\]](#); N. Brambilla, J. Ghiglieri, P. Petreczky, and A. Vairo, *Phys.Rev.* **D82**, 074019 (2010), [arXiv:1007.5172 \[hep-ph\]](#).
- [27] A. Adare *et al.* (PHENIX Collaboration), *Phys.Rev.* **D86**, 072008 (2012), [arXiv:1205.5533 \[hep-ex\]](#).